

A Microbial Electrochemical Technology to Detect and Degrade Organophosphate Pesticides

Amruta A. Karbelkar, Erin E. Reynolds,[‡] Rachel Ahlmark,[‡] and Ariel L. Furst^{*}Cite This: *ACS Cent. Sci.* 2021, 7, 1718–1727

Read Online

ACCESS |



Metrics & More

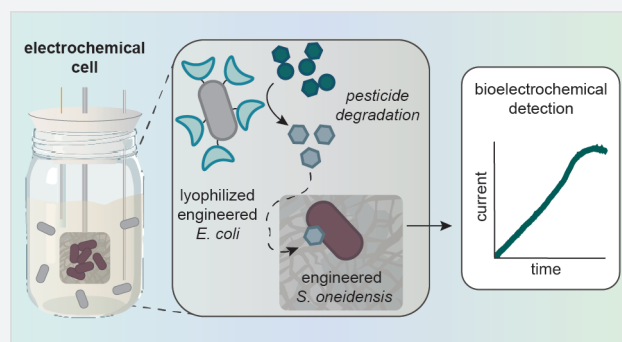


Article Recommendations



Supporting Information

ABSTRACT: Organophosphate (OP) pesticides cause hundreds of illnesses and deaths annually. Unfortunately, exposures are often detected by monitoring degradation products in blood and urine, with few effective methods for detection and remediation at the point of dispersal. We have developed an innovative strategy to remediate these compounds: an engineered microbial technology for the targeted detection and destruction of OP pesticides. This system is based upon microbial electrochemistry using two engineered strains. The strains are combined such that the first microbe (*E. coli*) degrades the pesticide, while the second (*S. oneidensis*) generates current in response to the degradation product without requiring external electrochemical stimulus or labels. This cellular technology is unique in that the *E. coli* serves only as an inert scaffold for enzymes to degrade OPs, circumventing a fundamental requirement of coculture design: maintaining the viability of two microbial strains simultaneously. With this platform, we can detect OP degradation products at submicromolar levels, outperforming reported colorimetric and fluorescence sensors. Importantly, this approach affords a modular, adaptable strategy that can be expanded to additional environmental contaminants.



INTRODUCTION

The organophosphate (OP) pesticides parathion and paraoxon cause thousands of illnesses and deaths annually, as they have the same mechanism of action as the nerve gas sarin.^{1–4} Such compounds disrupt the native neurotransmitter acetylcholine^{5,6} and impact the parasympathetic nerve system, which can be deadly.^{1–4} Similar compounds were employed as chemical weapons during World War II in the form of sarin, cyclosarin, and soman. OP chemical warfare agents (CWAs) have continued to be used as recently as 2017.¹ However, the main application of OPs is not as CWAs but as insecticides and pesticides.^{2–4,7–9} In fact, OPs are the most widely used pesticides in industrialized countries, causing environmental contamination and posing significant danger following exposure.¹⁰ Annually, there are an estimated three million exposures to OPs, causing 300 000 fatalities.^{11–13} The continued danger of these pesticides necessitates vigilance and affordable, easy-to-use technologies for detection and remediation, especially in low-resource settings.

Although physical and chemical decontamination strategies have been developed for the capture or degradation of OPs,¹ enzymatic methods are popular due to their substrate promiscuity, ability to directly degrade these compounds, and ready incorporation into genetically modified organisms (GMOs). Organophosphate hydrolases (OPHs) are extensively used because of their compatibility with recombinant expression and with incorporation into biomaterials.^{1,14,15}

However, OPH can be challenging to work with due to its tendency to aggregate.^{16–18} Polymer encapsulation has been used to improve protein stability and delivery^{19–31} but still requires challenging protein isolation and purification prior to deployment.

Significant effort has been devoted to whole cell-based remediation, including the application of microbes that natively express OPH^{32–37} and *E. coli*^{38–41} engineered to express it.⁴² However, these engineered cells must be viable and therefore require a bioreactor for remediation, which can be challenging to maintain. Though these cell-based methods have provided a solid foundation for OP remediation, they remain limited due to the necessity of maintaining viable cells, the energetic cost to cells of expressing the proteins, and the regulatory limits on the distribution of living GMOs.

Just as with OP degradation, many physical and chemical methods exist to detect OPs, including mass spectrometry.^{43,44} However, these methods are challenging to implement at the point-of-exposure due to their high cost and significant

Received: August 2, 2021

Published: September 21, 2021



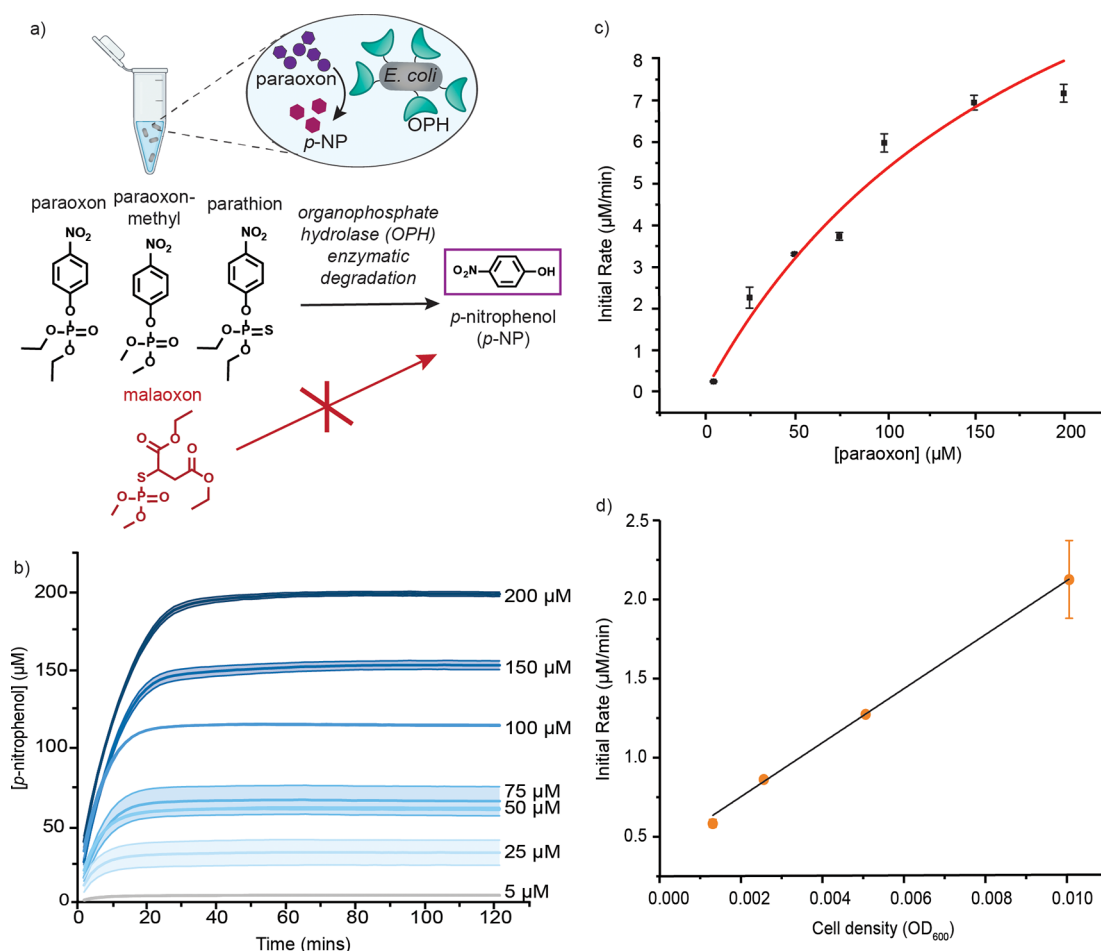


Figure 1. Degradation of organophosphates (OPs) by engineered *E. coli*. (a) Schematic representation of paraoxon degradation to *p*-nitrophenol (*p*-NP) by organophosphate hydrolase (OPH)-expressing *E. coli* and structures of OPs analyzed in this study, namely, paraoxon, paraoxon-methyl, parathion, and malaoxon. (b) Production of *p*-NP over time by OPH-expressing *E. coli* at different paraoxon concentrations, ranging from 5 to 200 μM . (c) Effect of paraoxon concentration on the initial rate of *p*-NP production, fitted with Michaelis–Menten equation (red). (d) Effect of OPH-expressing *E. coli* cell concentration (expressed in terms of OD_{600}) on the initial rate of *p*-NP production, fitted with a linear regression line, $R^2 = 0.99$ (black). Error bars represent SD for $n = 3$ biological replicates.

instrumentation requirements. Thus, the majority of effort devoted to sensing these compounds has focused on the development of biosensors with optical or electrochemical readout. Most often, detection is accomplished through the biological degradation of OPs followed by monitoring of the degradation products.^{33,40,45–53} These strategies are aided by the fact that the paraoxon and parathion degrade to *p*-nitrophenol (*p*-NP), which is both UV absorbent and electroactive. However, relying on the direct detection of *p*-NP poses challenges for detection in complex matrices, as naturally-occurring phenols can confound signals.

To increase the specificity of detection, biosensors employing specific recognition elements are advantageous. Engineered microbes offer a promising platform for such sensing because they can metabolize a broad range of chemicals, adopt emergent abilities, tolerate genetic modifications through recombinant DNA methods, and serve as a source of enzymes.⁵⁴ Because of their tolerance for nonideal environmental conditions and ability to serve as a sensor for both the toxicity and the bioavailability of targets, microbial biosensors are often used for environmental monitoring.⁵⁵ One main challenge with microbial biosensors is that they generally rely on visual readout (colorimetric,⁵⁶ fluorescent,^{57,58} or bio-

luminescent⁵⁹), making quantitative measurements at the point-of-contamination challenging.

Here, we report an engineered dual species technology for the targeted detection and destruction of parathion-type OPs. This technology is based on electrochemical signals generated by electroactive microbes in response to OP degradation products. Electroactive microbes generate current through extracellular electron transfer (EET) by supplying their metabolic electrons to an external electron acceptor, such as a poised electrode. *S. oneidensis* and similar microbes use multiheme cytochrome protein conduits spanning from the inner to the outer membrane and diffusible redox mediators to directly or indirectly perform EET.^{60–63} The first microbe in our technology, *E. coli*, degrades the pesticide, while the second (*S. oneidensis*) generates current in response to the degradation product without external electrochemical stimulus or labels. This cell mixture is unique in that enzymes displayed on *E. coli* function even when the cells are lyophilized,⁶⁴ enabling the cells to serve only as an inert scaffold and circumventing a core challenge in coculture design: maintaining the viability of two microbial strains simultaneously. Using this engineered microbial system, we have demonstrated the detection of OP degradation products at submicromolar levels, outperforming

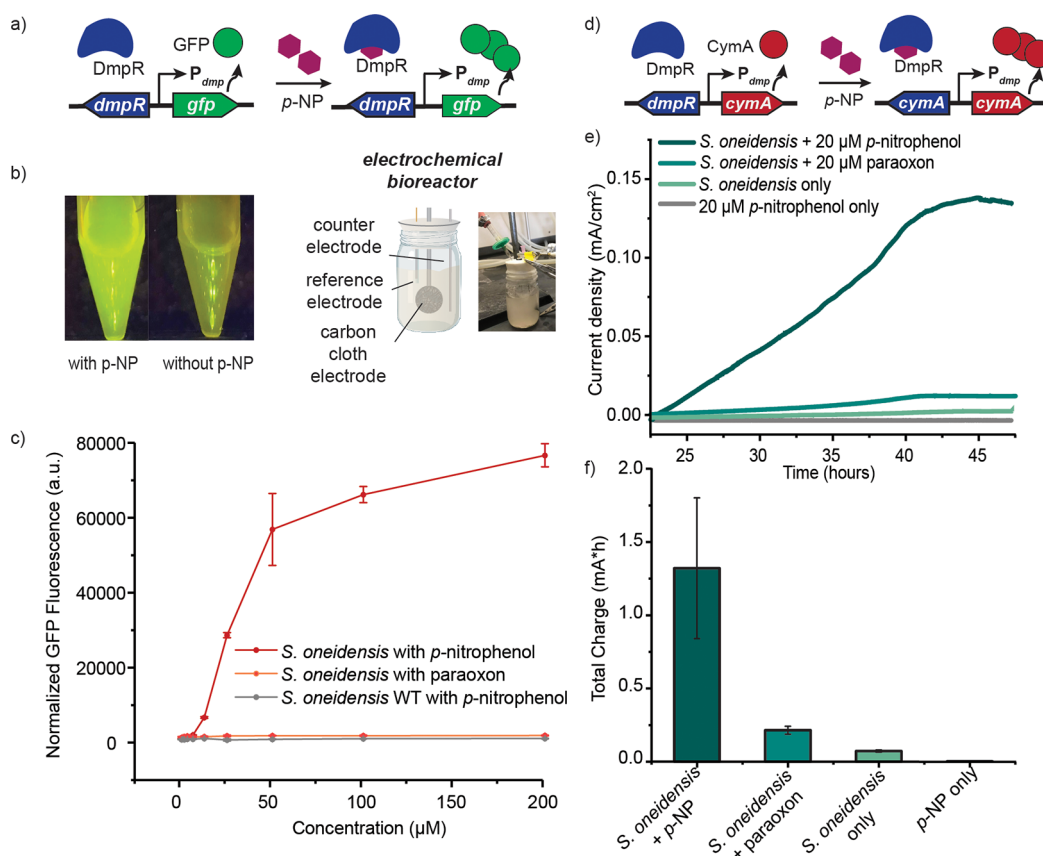


Figure 2. Detection of organophosphate (OP) degradation product, *p*-nitrophenol (*p*-NP) by engineered *S. oneidensis*. (a) Scheme depicting the genetic circuit engineered in *S. oneidensis* in which *p*-NP binds to the transcription factor DmpR, inducing the expression of green fluorescent protein (GFP). (b) GFP fluorescence in *S. oneidensis* cultures with and without the inducer, *p*-NP (left). Scheme depicting an electrochemical bioreactor setup containing carbon cloth working electrode, Pt counter electrode, and AgCl/Ag reference electrode (right). (c) GFP fluorescence normalized to OD₆₀₀ produced by engineered *S. oneidensis* in response to different concentrations of *p*-NP (red) and paraoxon (light red), and by wild-type *S. oneidensis* cells with different *p*-NP concentrations (gray) after 24 h induction. (d) Scheme depicting genetic circuit engineered in *S. oneidensis* in which *p*-NP binds to DmpR, inducing the expression of CymA, a critical extracellular electron transfer protein in *S. oneidensis*. (e) Representative chronoamperometry plots indicating the change in current density over time in bioreactors containing engineered *S. oneidensis* cells with 20 μM *p*-NP (dark green), cells with 20 μM paraoxon (teal), cells without any inducer (light green), and 20 μM *p*-NP without cells (gray). (f) Total charge produced by the cells in 24 h during chronoamperometry experiments under varying conditions. Error bars represent SD for $n = 3$ biological replicates.

reported absorbance and fluorescence sensors.⁶⁵ Our approach affords a modular, adaptable strategy through dual microbial engineering to control electron transfer in one organism with molecules generated from contaminant degradation by another.

RESULTS

Degradation of Organophosphates Using Engineered *E. coli*. We have used the surface of *E. coli* as a platform to display organophosphate hydrolase (OPH) for OP degradation. The OPH used in this study is a phosphotriesterase obtained from *Pseudomonas diminuta*.⁶⁶ Also known as parathion hydrolase, the enzyme specifically degrades synthetic OP triesters and phosphorofluoridates with high catalytic efficiency.⁶⁶ With its ability to efficiently degrade these toxic compounds, this OPH has been widely used for remediation purposes.^{10,11,33} Using our previously-reported strategy employing the INPNC ice-nucleation sequence, OPH was displayed on the cell surface.⁶⁴ The ice-nucleation sequence circumvents the cytotoxic effects of the more common surface expression tag, OmpA.³⁹ Moreover, the cells are lyophilized following OPH expression, making their viability unnecessary

for OP degradation and potentially increasing the length of their storage life⁶⁷—both important for an optimal deployable technology. Extrapolating from previous INPNC *E. coli* expression, we estimate approximately 50 000 enzymes to be expressed per lyophilized cell using our induction conditions.⁶⁴

The degradation of paraoxon by lyophilized OPH-*E. coli* was confirmed by monitoring the OP degradation product, *p*-NP, using a colorimetric assay (Figure 1).⁶⁶ Under alkaline conditions, *p*-NP forms a phenolate ion, which is yellow in color and has a maximum absorbance at 400 nm.⁶⁸ The absorbance values obtained from the colorimetric assay were converted to *p*-NP concentrations with the help of a standard curve. We can therefore quantify paraoxon degradation through the production of *p*-NP at a fixed cell density (OD₆₀₀ 0.02) (Figure 1b). At each paraoxon concentration, rapid initial *p*-NP production followed by equilibration was observed. From these data, enzyme kinetic parameters were determined by fitting the Michaelis–Menten equation (Figure 1c). The Michaelis constant (K_M) of paraoxon for the enzyme was calculated to be $197.9 \pm 81.7 \mu\text{M}$, which is slightly higher than the reported affinity of paraoxon for purified OPH.⁶⁶ This is hypothesized to be due to restricted substrate diffusion to

the enzymes that are confined on the cells rather than free in solution.⁶⁹ To determine the effect of enzyme concentration on substrate turnover, a fixed concentration of paraoxon was added to varying concentrations of lyophilized OPH-*E. coli* (Figure S1). As anticipated, the initial reaction rate of paraoxon degradation is directly proportional to the cell concentration, and therefore, the OPH enzymes expressed on the *E. coli* cell surface (Figure 1d). These results indicate that the OPH enzymes on the surface of *E. coli* retain their biologically-relevant conformation even following lyophilization. The degradation of paraoxon, therefore, does not require viable *E. coli* to proceed.

To evaluate the generalizability of this biomaterial for OP remediation, we tested additional organophosphates. Parathion is another especially common OP pesticide, but it contains a phosphorus–sulfur bond in place of the phosphorus–oxygen bond found in paraoxon. We evaluated the ability of our OPH-*E. coli* to degrade parathion and observed similar results to paraoxon degradation (Figure S2a, c). The catalytic efficiency (V_{\max}/K_M) is $0.079 \pm 0.13 \text{ min}^{-1}$ for paraoxon and $0.104 \text{ min}^{-1} \pm 0.013$ for parathion. Previous reports suggest that paraoxon slightly outperforms parathion as a substrate for the OPH enzyme,⁶⁶ though our analysis does not show a significant difference between the two. We further evaluated the degradation of paraoxon-methyl, which differs from paraoxon in the substituents on the phosphate. Under the same experimental conditions, very slow rates of *p*-NP production were observed, and the rate did not reach equilibrium even after 2 h. Upon reducing the concentration of the solvent methanol from 0.1% to 0.01%, significantly enhanced degradation rates for paraoxon-methyl were observed (Figure S2b, d), indicating enzyme inhibition by methanol. Polar solvents have been suggested to competitively inhibit the OPH active site.⁷⁰ Taken in total, our results demonstrate that the OPH expressed on *E. coli* can degrade a variety of OPs, albeit with differing efficiencies.

Fluorescent Detection of the Organophosphate Degradation Product *p*-NP by Engineered *S. oneidensis*.

Electrochemical sensors to detect OP pesticides most often rely on the direct detection of *p*-NP. However, off-target phenols that are common in environmental matrices can have similar electrochemical properties, causing false positive results. To enhance the specificity and sensitivity of our biosensing system, we engineered the electroactive microbe *S. oneidensis* such that the expression of EET machinery, and hence current production, is triggered by *p*-NP. A phenol-responsive transcription factor, DmpR (dimethyl phenol regulator) from *Pseudomonas* spp. CF600, is known to undergo a conformational change upon interaction with a phenol such as *p*-NP, activating the DmpR promoter, P_{dmp} .⁷¹ To determine whether DmpR responds to *p*-NP, we initially placed the induction of green fluorescent protein (GFP) under the control of P_{dmp} in both *S. oneidensis* and *E. coli* (Figure 2a), as GFP fluorescence facilitated high-throughput analysis. In the engineered *S. oneidensis*, a 54-fold increase in fluorescence was observed with 200 μM *p*-NP, with fluorescence observed at *p*-NP concentrations as low as 6.25 μM (Figure 2b,c). Further, gene expression was found to be logarithmic, showing a sharp increase in fluorescence at 6.25 μM *p*-NP, which nearly levels off at concentrations higher than 50 μM . No such increase in the fluorescence was observed for wildtype (WT) *S. oneidensis* following the addition of paraoxon. *E. coli* similarly displayed a logarithmic increase in GFP expression upon a *p*-NP

concentration increase from 6.25 to 50 μM (Figure S3). This response was significantly higher than for WT *E. coli* treated with *p*-NP or GFP-expressing cells treated with paraoxon. These results confirm that the transcription factor, DmpR, in the engineered cells is responsive to the inducer *p*-NP. Further, this response is specific to the OP degradation product, not to the OP itself.

To confirm the specificity of DmpR for *p*-NP and not off-target phenols found in natural systems, we performed a GFP assay on off-target compounds. By exposing the engineered *p*-NP-responsive *S. oneidensis* to different concentrations of three environmentally-relevant off-target compounds (dopamine, hydroquinone, and 4-methylcatechol), the specificity of this transcription factor was confirmed. Compared to the normalized GFP fluorescence emissions of *p*-NP, the off-target compounds produced very low fluorescence, providing further evidence for the specificity of the sensor and its viability for field deployment (Figure S4).

Electrochemical Detection of *p*-NP by Engineered *S. oneidensis*.

We next evaluated whether *p*-NP-activated DmpR can elicit an electrochemical response in *S. oneidensis*. Here, we placed expression of an inner membrane-bound EET protein, CymA, under control of P_{dmp} . CymA is a tetraheme quinol dehydrogenase responsible for directing metabolic electron flux to the extracellular space through the MtrABC conduit.⁶⁰ CymA was selected over other Mtr proteins (MtrB and MtrC), as we observed highest induction and minimal leakiness in the IPTG-inducible knockout strains that were used to construct the *p*-NP-inducible strains. Constitutively-expressed DmpR activates P_{dmp} in the presence of *p*-NP, leading to the expression of CymA (Figure 2d), which “completes the circuit” and enables EET in *S. oneidensis*. We validated this response by introducing the engineered cells to a three-electrode bioreactor consisting of a carbon cloth working electrode poised at +400 mV vs silver chloride/silver (AgCl/Ag) (Figure 2c). Cells were provided with lactate as an electron donor and carbon source, and the poised carbon cloth electrode is expected to function as an electron acceptor only in the presence of *p*-NP. The reactor headspace was open to the atmosphere to allow O_2 diffusion for cells to use as an alternate electron acceptor in the absence of *p*-NP.⁷² *S. oneidensis* can respire electrodes under low O_2 tension, indicating that the presence of O_2 does not hinder EET by the cells.⁷³ A continuous increase in anodic current, indicating electron transfer from cells to the electrode, was observed only following addition of *p*-NP to the bioreactor. Cells alone, *p*-NP alone, and cells with paraoxon did not yield a considerable current (Figure 2e, S5). At 20 μM *p*-NP, the cells generated a total charge of $1.32 \pm 0.48 \text{ mA}\cdot\text{h}$ in 24 h; the cells without *p*-NP added or with paraoxon added generated only $0.072 \pm 0.006 \text{ mA}\cdot\text{h}$ charge and $0.21 \pm 0.02 \text{ mA}\cdot\text{h}$ charge in the same amount of time, respectively (Figure 2f). The small current observed in the presence of paraoxon is likely due to low levels of its nonenzymatic degradation. Taken together, these results confirm that *p*-NP specifically leads to CymA expression, allowing the cells to perform EET to an external electrode. Overall, our fluorescence and electrochemical measurements indicate that the transcription factor DmpR is activated by the OP degradation product *p*-NP, which in turn induces the expression of target proteins (either GFP or CymA).

GFP Fluorescence Response of Engineered Cocultures to Organophosphates. After independently confirming OP degradation activity by lyophilized OPH-*E. coli* and *p*-

NP detection by engineered *S. oneidensis* in each monoculture, we assessed the activity of the two microbes together in the presence of OPs. For initial validation, we added lyophilized OPH-*E. coli* to DmpR-driven, GFP-expressing *S. oneidensis*. GFP fluorescence was monitored over time in the presence of paraoxon (Figure 3a). We observed an increase in GFP

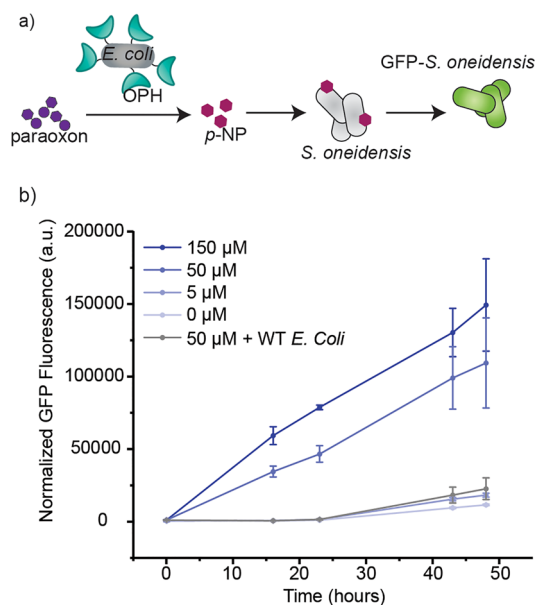


Figure 3. GFP fluorescence response of engineered cocultures to OPs. (a) Scheme depicting the degradation of paraoxon by OPH-expressing *E. coli* to produce *p*-NP, which is detected by engineered *S. oneidensis*, causing GFP expression in cells. (b) GFP fluorescence normalized to OD₆₀₀ produced over time by engineered cocultures in the presence of different initial concentrations of paraoxon, ranging from 0 to 150 μM and coculture with wild-type *E. coli* containing 50 μM paraoxon (gray). Error bars represent SD for *n* = 3 replicates.

fluorescence for cell mixtures with an initial paraoxon concentration of 5, 50, and 150 μM (Figure 3b), and the magnitude of the fluorescence was dependent on the initial OP concentration. From the time of inoculation to 24 h, a 55-fold increase in fluorescence was observed for cocultures with 150 μM paraoxon added; a 35-fold increase was observed with 50 μM paraoxon, and a 2.5-fold increase was observed with 5 μM paraoxon. Minimal fluorescence was observed in cocultures containing lyophilized WT *E. coli* in place of OPH-expressing *E. coli*. Similar degradation and detection efficiencies were observed in a dual *E. coli* system (OPH-*E. coli* and DmpR driven GFP expressing *E. coli*) (Figure S6). These results, combined with monoculture experiments, suggest that OPH-*E. coli*-mediated paraoxon degradation activates DmpR in engineered *S. oneidensis*, leading to an increase in GFP fluorescence over time. Furthermore, our results indicate that GFP induction by *p*-NP in engineered *S. oneidensis* is concentration dependent, enabling a quantitative measure of OP concentration.

Based on the initial success of the mixture, we investigated whether other OPs (paraoxon-methyl, parathion, and malaoxon) generate a GFP response in our lyophilized OPH-*E. coli* and engineered *S. oneidensis* combination. We found similar degradation and detection efficiencies with paraoxon-methyl, parathion, and paraoxon (Figure S7a,b). At 150 μM initial OP concentration, the mixtures with parathion generated a 58-fold

increase in fluorescence, and those with paraoxon-methyl generated a 48-fold increase within 24 h of inoculation. These results confirm that OPs that generate a *p*-NP degradation product elicit GFP expression in our engineered *S. oneidensis*. As a negative control, we evaluated malaoxon, which does not yield a phenolic degradation product. As predicted, GFP expression was not observed in our cell mixtures with malaoxon, further validating the specificity of the response (Figure S7c). Overall, our results confirm that the increase in fluorescence in OPH-*E. coli*/*S. oneidensis* mixtures is due to the degradation of OPs to *p*-NP, leading to GFP expression in *S. oneidensis*. Furthermore, this system functions for any OP substrate that is hydrolyzed to *p*-NP.

Electrochemical Response of Engineered Cocultures to Organophosphates.

To generate an electrochemical biosensor for OP detection and degradation, we combined *S. oneidensis* that expresses the critical EET protein CymA in response to *p*-NP with lyophilized OPH-*E. coli* (Figure 4a). The electrochemical response of engineered cell mixtures was measured in three-electrode bioreactors, identical to the monoculture experiments. An increase in anodic current was observed only following the addition of paraoxon to the bioreactor containing both lyophilized OPH-*E. coli* and engineered *S. oneidensis* (Figures 4b and S8). This increase was significantly higher than the current produced by either the cell mixture in the absence of paraoxon or the paraoxon alone, which generated current similar to that of the media baseline. The slight decrease in current density in the coculture reactors with paraoxon after 40 h could likely be due to electron donor depletion and is often observed in *S. oneidensis* bioreactors. The mixture with 20 μM paraoxon accumulated a total charge of 1.64 ± 0.18 mA·h in 24 h. In comparison, the cell mixture alone accumulated only 0.065 ± 0.002 mA·h of charge (Figure 4c). These results, combined with the observation that *S. oneidensis* monocultures produce anodic current only in the presence of *p*-NP, indicate that OPH-*E. coli*-mediated paraoxon hydrolysis leads to CymA expression in *S. oneidensis*, thereby initiating EET to the carbon cloth electrode. In agreement with our fluorescence experiments, we observed paraoxon-methyl and parathion yielded an increase in anodic current with the engineered cell mixtures. On the other hand, no significant current is observed with malaoxon, which does not generate *p*-NP (Figure S9). Comparable with paraoxon, in 24 h, we observed 1.03 ± 0.31 and 1.04 ± 0.66 mA·h charge with paraoxon-methyl and parathion, respectively, but only 0.068 ± 0.006 mA·h from malaoxon (Figure 4d), which is equivalent to the coculture only control. Our results consistently show that the current response is directly proportional to the initial concentration of paraoxon (Figure S10a). The total charge produced by the bioreactors was calculated at 5, 10, and 24 h (Figure 4e). Within 5 h, 20 μM paraoxon could be detected with charge accumulation of 0.140 ± 0.02 mA·h. At 24 h, the charge produced by the cell mixture with 5 μM paraoxon (0.180 ± 0.018 mA·h) was approximately three times higher and with 1 μM concentration (0.101 ± 0.017 mA·h) was 1.7 times higher than the cell only baseline. By determining the slope (*S*) and standard deviation of the intercept (*S*_y) from the linear fit of the calibration curve (Figure S10b), the limit of detection of the sensor was calculated to be $0.15 \mu\text{M}$ ($3.3 \times (S_y/S)$). Though we did not explicitly evaluate current generation as a function of *p*-NP concentration, we have demonstrated current generation to be the rate-limiting step for the degradation of paraoxon and

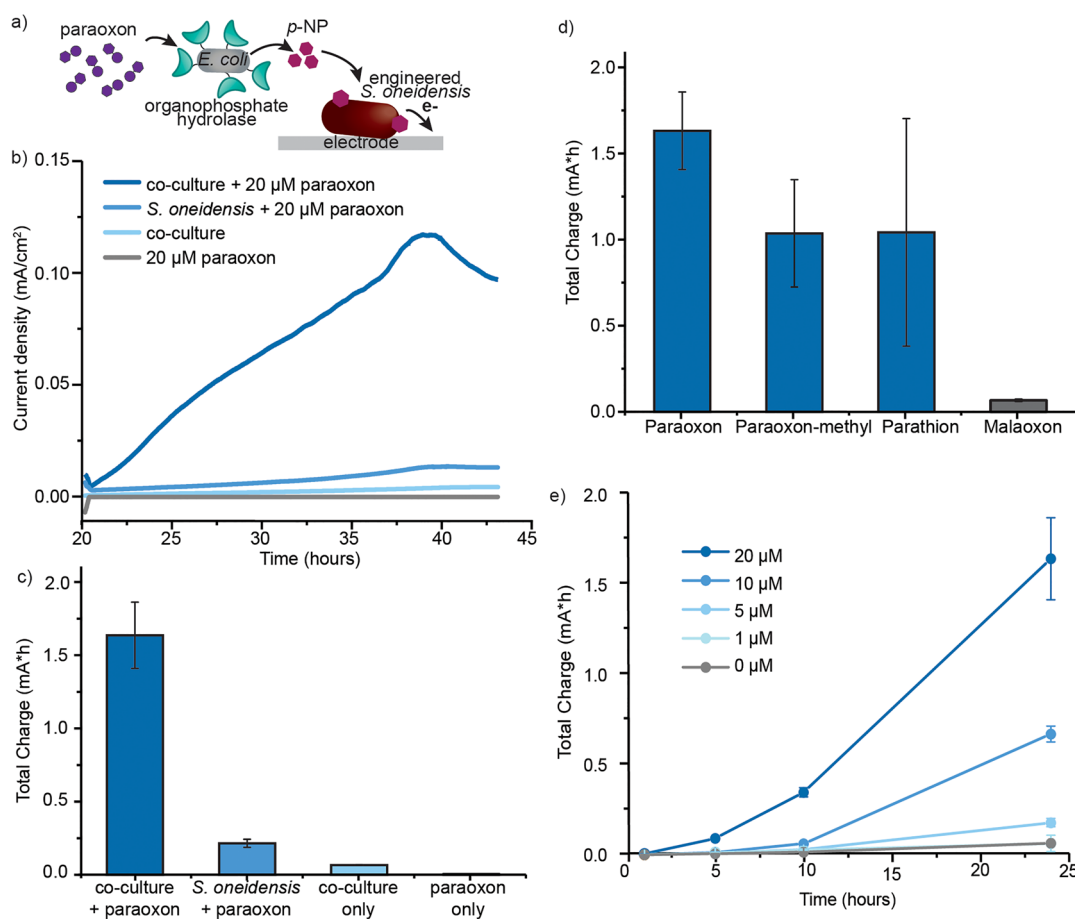


Figure 4. Electrochemical response of engineered cocultures to organophosphates. (a) Scheme depicting the degradation of paraoxon by OPH-expressing *E. coli* to *p*-NP, which further induces expression of CymA in engineered *S. oneidensis*, allowing EET from the cells to an external electrode. (b) Representative chronoamperometry plots indicating the change in current density over time in bioreactors containing engineered cocultures with 20 μM paraoxon (dark blue), *S. oneidensis* with 20 μM paraoxon (blue), coculture only (light blue) and 20 μM paraoxon without cells (gray). (c) Total charge produced by the cells in 24 h during chronoamperometry experiments under different conditions. (d) Total charge produced by the engineered cocultures in 24 h during chronoamperometry experiments in the presence of different organophosphates. (e) Total charge produced by the cocultures over time during chronoamperometry experiments with different initial paraoxon concentrations ranging from 0 to 20 μM. Error bars represent SD for $n = 3$ replicates.

detection of *p*-NP. Thus, we expect similar results for the direct detection of *p*-NP to those observed with varying paraoxon concentrations, in which a linear range of detection is observed between 5 and 20 μM (Figure S10). Our electrochemical measurements thus confirm that this technology is sensitive and specific. Further, it is capable of degradation and detection of toxic OPs in a single assay.

DISCUSSION

In this study, we have shown that engineered microbial combinations can both degrade and detect toxic OPs with incomparable specificity and sensitivity using electrochemical readout.^{1,33,40,45–53,65} *E. coli* were engineered to express OPH on the cell surface to degrade organophosphate pesticides to *p*-NP, even following *E. coli* lyophilization. We also engineered electroactive microbes, *S. oneidensis*, to express a critical EET protein, CymA, in the presence of *p*-NP. Expression of CymA completes the electron transfer pathway, allowing the bacteria to respire external electrodes. After validating the function of the two engineered microbes individually, our coculture studies confirm that OPH-expressing *E. coli* degrade OPs and that *S. oneidensis* detect the degradation product and generate current as a readout in a single assay.

The state-of-the-art for OP remediation and biosensing relies on assays that either degrade or detect the OPs. Using our engineered bacterial cell mixture, our electrochemical assay can perform both functions in a single system. OPH had previously been used to enzymatically degrade OPs, but these technologies suffer from OPH instability. Expression of this enzyme on the *E. coli* surface circumvents difficulties with protein handling. Further, our OPH-expressing *E. coli* are lyophilized, yet they maintain their enzymatic degradation activity. This is an important development, as we have bypassed the need to develop optimal culture conditions for two microbes to maintain metabolic activity in coculture. Lyophilization also allows for long-term storage of the enzyme-modified *E. coli*,⁶⁴ making them highly suitable for field-based OP biosensing and remediation.

Often, electrochemical OP detection depends upon the direct sensing of *p*-NP. Previously, amperometric biosensors using gold–titanium oxide electrodes modified with horse radish peroxidase and methylene blue have resulted in exceptional sensitivity toward the detection of *p*-NP.⁷⁴ However, other phenolic compounds interact with this platform, which can compromise its specificity. Additionally, a low-cost 3D paper based electrochemical sensor for *p*-NP,

with combined filtration and detection, has been reported.⁷⁵ As the detection is based upon physical electrostatic interactions between the electrode and the analyte, the response is negatively impacted at more relevant neutral/near-neutral pH. While the authors demonstrate *p*-NP specificity among other contaminants with distinct electrochemical signatures, the response may become convoluted for compounds with redox properties similar to *p*-NP. This can lead to low specificity and false positives, as other species with similar electrochemical properties can trigger an electrochemical response. With our engineered *S. oneidensis*, the current is specific to the presence of *p*-NP, and thus the possibility of false positives is minimized. EET in the bacteria is “turned-on” only in its presence. Another clever nanocatalyst-based electrochemical immunosensor was developed for the ultra-sensitive detection of *p*-NP,⁷⁶ but the sensor fabrication requires extensive electrode surface modification, labeling, and the use of antibodies, which impacts the cost and stability of this platform. In contrast, by using our whole cell-based assay with lyophilized bacteria, we anticipate that our biosensing strategy can be used as a cheap and robust system for field deployment. Overall, our engineered microbes have streamlined OP biodegradation and biosensing in a single system. This technology provides a significant improvement over the current biosensors in terms of handling, storage, and specificity.

Our electrochemical cell system enables continuous monitoring without the need for sampling or sample processing, as is required for fluorescence-based assays. The current study provides a proof-of-principle for the two engineered microbes to simultaneously degrade and detect dangerous, environmental contaminants. Improving the fitness of the transcription factor DmpR for enhanced interaction with *p*-NP could result in faster *p*-NP detection and response times by *S. oneidensis*. Additionally, since this strategy requires only *S. oneidensis* to be viable, the biosensor can easily be deployed for long-term, autonomous monitoring, merely by varying the ratio of the two bacteria, without the need for reoptimization. Overall, we have demonstrated and verified a unique electrochemical OP biosensing strategy based on engineered *E. coli* and *S. oneidensis* to degrade and detect highly toxic OPs in a single assay.

With the continued use of OP pesticides despite their toxicity, technologies to detect and degrade these chemicals are desperately needed. Our engineered cell mixture combined with electrochemical readout is the first example of a technology for specific recognition and destruction of this class of harmful compounds. Electrochemistry provides high sensitivity at a low cost, and engineered microbes offer unparalleled specificity. This work represents a paradigm shift in sensing and remediation through dual microbial engineering to control electron transfer in one organism with molecules generated from degradation by the other. Importantly, we anticipate this modular assembly to be readily applied to other classes of harmful contaminants.

■ MATERIALS AND METHODS

Strain Engineering. *OPH Sequence.* The organophosphate hydrolase (OPH) sequence used was parathion hydrolase from *Pseudomonas diminuta* (Uniprot ID: P0A434). The sequence was codon-optimized for expression in *E. coli* and cloning-relevant restriction sites were removed. The OPH gene was synthesized by Twist Bioscience (South San Francisco,

CA) as a fusion with the INPNC ice-nucleation sequence⁶⁴ on the N-terminus.

OPH-E. coli. The INPNC-OPH fusion was cloned into plasmid backbone pSKB3, previously described in ref 64. pSKB3 is a variation of Novagen's pET-28a vector with the thrombin site exchanged for a TEV proteolysis site. The vector (pSKB3) and the insert (INPNC-OPH) were double digested with *Xho*I and *Nco*I for 35 min at 37 °C. Digestion products were run on a TAE 1.6% agarose gel at 100 V for 30 min. Desired fragments were gel extracted using the Zymoclean Gel DNA Recovery Kit (Zymo Research). Purified DNA fragments were ligated using T4 DNA Ligase (NEB M0202). A 1:3 molar ratio of vector to insert and 50 ng of vector was used. The ligation mixture was transformed into chemically-competent DH5 α *E. coli* and plated on LB-agar kanamycin plates to select for positive transformants. A single colony was picked from the agar plate, inoculated in 5 mL LB-kanamycin, grown in a shaking incubator (250 rpm) for at least 16 h at 37 °C, and miniprep using QIAprep Spin Miniprep Kit (Qiagen). The plasmid DNA was sequence-verified by sample submission to Genewiz (Cambridge, MA). Subsequently, the plasmid was transformed into chemically-competent BL21(DE3) *E. coli* to create the surface-expressed OPH-*E. coli* strain.

DmpR and P_{DmpR} Sequences. The sequence used for the *p*-NP-responsive transcription factor DmpR (dimethyl phenol regulator) was obtained from *Pseudomonas* spp. CF600 (Uniprot ID: Q06573). This sequence was modified with mutations Q10R and K117M because these mutations had been shown to improve the responsiveness of this transcription factor toward *p*-NP by 7-fold over the native protein.⁷¹ The promoter sequence recognized by DmpR (P_{DmpR}) was obtained from the iGEM Registry of Standard Biological Parts. P_{DmpR} in our plasmid maps is identical to the Po promoter sequence including the ribosome binding site B0031 in part BBa_K1031221. DmpR and P_{DmpR} sequences were codon-optimized for expression in *S. oneidensis* and synthesized by Twist Bioscience (South San Francisco, CA).

Preparation of Lyophilized *E. coli*. *E. coli* (engineered or wild-type) was grown overnight for 18–20 h in 5 mL LB supplemented with 50 μ g/mL kanamycin at 37 °C and 200 rpm from 25% frozen glycerol stocks (stored at –80 °C). The preculture was diluted to 0.1 OD₆₀₀ in 20 mL Terrific Broth (TB) supplemented with potassium phosphate buffer (17 mM KH₂PO₄, 72 mM K₂HPO₄), 0.5% glucose, and 50 μ g/mL kanamycin. The culture was incubated at 37 °C and 200 rpm until OD₆₀₀ was approximately 0.8. The culture was induced using 100 μ M IPTG and incubated at 18 °C, 200 rpm for 20 h. The cells were pelleted by centrifugation at 8942 \times g for 3 min. The supernatant was discarded, and cells were washed twice by centrifugation and resuspension in a defined media. After the final wash, cells were diluted in the same defined media with 100 mM trehalose as a cryoprotectant to a final OD₆₀₀ of 0.1 or 2.0, depending upon the use. The defined media for resuspension was phosphate citrate buffer (pH 8.0) for colorimetric assays, phosphate buffered saline (pH 7.4) for fluorescence assays and M1 minimal media (pH 7.0) for electrochemical measurements. One mL aliquots of the cell culture at specific OD₆₀₀ were flash frozen with liquid N₂, lyophilized under vacuum and stored at –20 °C until further use. Before use, the lyophilized cells were reconstituted in sterile water.

Bioelectrochemical Measurements. *Electrochemical Analysis.* The electrochemical measurements were performed

in a single-chamber, three electrode bioreactor consisting of 1 cm² PW06 carbon cloth (Zoltek, St. Louis, MO) as a working electrode, Pt wire (Sigma-Aldrich) as a counter electrode, and AgCl/Ag (CH Instruments, Austin, TX, USA) as a reference electrode. A 90 mL portion of M1 media modified from previous reports⁷⁷ was used for the electrode cultivation of *S. oneidensis*. The cells were provided with 18 mM sodium lactate as a carbon and electron source. The media was further supplemented with vitamins, minerals, and amino acids as previously reported.⁷⁷ Riboflavin was, however, excluded from the vitamin solution to avoid riboflavin-induced electrochemical signals. The reactors were sealed with a rubber stopper with two needles to allow minimal air diffusion. Chronoamperometry measurements were made using a 16-channel potentiostat (Biologic, Seyssinet-Pariset, France) or a 4-channel potentiostat (Admiral Instruments, Tempe, AZ). The working electrode potential was maintained at 0.4 V vs AgCl/Ag reference electrode, thereby acting as an electron sink for the bacteria. A baseline current was first obtained at the applied potential prior to *S. oneidensis* inoculation. To study the effect of *p*-NP on the engineered *S. oneidensis* strain, the cells were first inoculated in the bioreactor to a final OD₆₀₀ of 0.8, followed by an injection of *p*-NP to a final concentration of 20 μM, at an interval of 1 h. For coculture experiments, after an hour of *S. oneidensis* inoculation, 1 mL of lyophilized *E. coli* cells in M1 media were resuspended in sterile water and added to the bioreactor to a final OD₆₀₀ of 0.02. After another hour, the OP at the desired final concentration was injected. The current was measured for 24 h after the *p*-nitrophenol or OP injection and normalized to the projected surface area of the carbon cloth electrode. The total charge produced by *p*-NP, or OP was determined by computing the area under the chronoamperometry curve from their time of introduction in the bioreactor up to 24 h using OriginLab data analysis software (Northampton, MA).

■ ASSOCIATED CONTENT

SI Supporting Information

The Supporting Information is available free of charge at <https://pubs.acs.org/doi/10.1021/acscentsci.1c00931>.

Strain engineering, colorimetric assay for organophosphate degradation using lyophilized OPH-*E. coli*, GFP fluorescence assay for monoculture and coculture experiments, bioelectrochemical measurements, and supplemental figures (PDF)

■ AUTHOR INFORMATION

Corresponding Author

Arnel L. Furst – Department of Chemical Engineering, Massachusetts Institute of Technology, Cambridge, Massachusetts 02139, United States; Center for Environmental Health Sciences, Massachusetts Institute of Technology, Cambridge, Massachusetts 02139, United States; orcid.org/0000-0001-9583-9703; Email: afurst@mit.edu

Authors

Amruta A. Karbelkar – Department of Chemical Engineering, Massachusetts Institute of Technology, Cambridge, Massachusetts 02139, United States

Erin E. Reynolds – Department of Chemical Engineering, Massachusetts Institute of Technology, Cambridge, Massachusetts 02139, United States

Rachel Ahlmark – Department of Chemical Engineering, Massachusetts Institute of Technology, Cambridge, Massachusetts 02139, United States

Complete contact information is available at:

<https://pubs.acs.org/10.1021/acscentsci.1c00931>

Author Contributions

[‡]E.E.R. and R.A. contributed equally.

Notes

The authors declare no competing financial interest.

■ ACKNOWLEDGMENTS

We would like to acknowledge the MIT J-WAFS program and the MIT Research Support Committee for supporting this work. Support for this research was also provided by a core center grant P30-ES002109 from the National Institute of Environmental Health Sciences, National Institutes of Health. We thank Prof. B. K. Keitz (University of Texas at Austin) for providing the Δ *cymA* *S. oneidensis* strain.

■ REFERENCES

- (1) Thakur, M.; Medintz, I. L.; Walper, S. A. Enzymatic Bioremediation of Organophosphate Compounds—Progress and Remaining Challenges. *Front. Bioeng. Biotechnol.* **2019**, *7*, 289.
- (2) DuBois, K. P.; Doull, J.; Salerno, P. R.; Coon, J. M. Studies on the Toxicity and Mechanism of Action of *p*-Nitrophenyl Diethyl Thionophosphate (Parathion). *J. Pharmacol. Exp. Ther.* **1949**, *95* (1), 79–91.
- (3) Stokes, L.; Stark, A.; Marshall, E.; Narang, A. Neurotoxicity among Pesticide Applicators Exposed to Organophosphates. *Occup. Environ. Med.* **1995**, *52* (10), 648–653.
- (4) Ruckart, P. Z.; Kakolewski, K.; Bove, F. J.; Kaye, W. E. Long-Term Neurobehavioral Health Effects of Methyl Parathion Exposure in Children in Mississippi and Ohio. *Environ. Health Perspect.* **2004**, *112* (1), 46–51.
- (5) Costa, L. G. Organophosphorus Compounds at 80: Some Old and New Issues. *Toxicol. Sci.* **2018**, *162* (1), 24–35.
- (6) Franjesevic, A. J.; Sillart, S. B.; Beck, J. M.; Vyas, S.; Callam, C. S.; Hadad, C. M. Resurrection and Reactivation of Acetylcholinesterase and Butyrylcholinesterase. *Chem. - Eur. J.* **2019**, *25* (21), 5337–5371.
- (7) Takamiya, K. Monitoring of Urinary Alkyl Phosphates in Pest Control Operators Exposed to Various Organophosphorus Insecticides. *Bull. Environ. Contam. Toxicol.* **1994**, *52* (2), 190–195.
- (8) Heudorf, U.; Angerer, J. Metabolites of Organophosphorous Insecticides in Urine Specimens from Inhabitants of a Residential Area. *Environ. Res.* **2001**, *86* (1), 80–87.
- (9) Arcury, T. A.; Grzywacz, J. G.; Davis, S. W.; Barr, D. B.; Quandt, S. A. Organophosphorus Pesticide Urinary Metabolite Levels of Children in Farmworker Households in Eastern North Carolina. *Am. J. Ind. Med.* **2006**, *49* (9), 751–760.
- (10) Hertz-Picciotto, I.; Sass, J. B.; Engel, S.; Bennett, D. H.; Bradman, A.; Eskenazi, B.; Lanphear, B.; Whyatt, R. Organophosphate Exposures during Pregnancy and Child Neurodevelopment: Recommendations for Essential Policy Reforms. *PLoS Med.* **2018**, *15* (10), e1002671.
- (11) Eddleston, M.; Phillips, M. R. Self Poisoning with Pesticides. *BMJ.* **2004**, *328* (7430), 42–44.
- (12) Eyer, P. The Role of Oximes in the Management of Organophosphorus Pesticide Poisoning. *Toxicol. Rev.* **2003**, *22* (3), 165–190.
- (13) Karunarathne, A.; Gunnell, D.; Konradsen, F.; Eddleston, M. How Many Premature Deaths from Pesticide Suicide Have Occurred

since the Agricultural Green Revolution? *Clin. Toxicol.* **2020**, *58* (4), 227–232.

(14) Flounders, A. W.; Singh, A. K.; Volponi, J. V.; Carichner, S. C.; Wally, K.; Simonian, A. S.; Wild, J. R.; Schoeniger, J. S. Development of Sensors for Direct Detection of Organophosphates: Part II: Sol-Gel Modified Field Effect Transistor with Immobilized Organophosphate Hydrolase. *Biosens. Bioelectron.* **1999**, *14* (8), 715–722.

(15) Del Giudice, I.; Coppolecchia, R.; Merone, L.; Porzio, E.; Carusone, T. M.; Mandrich, L.; Worek, F.; Manco, G. An Efficient Thermostable Organophosphate Hydrolase and Its Application in Pesticide Decontamination. *Biotechnol. Bioeng.* **2016**, *113* (4), 724–734.

(16) Gopal, S.; Rastogi, V.; Ashman, W.; Mulbry, W. Mutagenesis of Organophosphorus Hydrolase to Enhance Hydrolysis of the Nerve Agent VX. *Biochem. Biophys. Res. Commun.* **2000**, *279* (2), 516–519.

(17) Rastogi, V. K.; Defrank, J. J.; Cheng, T.; Wild, J. R. Enzymatic Hydrolysis of Russian-VX by Organophosphorus Hydrolase. *Biochem. Biophys. Res. Commun.* **1997**, *241* (2), 294–296.

(18) Kim, M.; Gkikas, M.; Huang, A.; Kang, J. W.; Suthiwangcharoen, N.; Nagarajan, R.; Olsen, B. D. Enhanced Activity and Stability of Organophosphorus Hydrolase via Interaction with an Amphiphilic Polymer. *Chem. Commun.* **2014**, *50* (40), 5345–5348.

(19) LeJeune, K. E.; Wild, J. R.; Russell, A. J. Nerve Agents Degraded by Enzymatic Foams. *Nature* **1998**, *395* (6697), 27–28.

(20) Lu, H. D.; Wheeldon, I. R.; Banta, S. Catalytic Biomaterials: Engineering Organophosphate Hydrolase to Form Self-Assembling Enzymatic Hydrogels. *Protein Eng., Des. Sel.* **2010**, *23* (7), 559–566.

(21) Lee, Y.; Stanish, I.; Rastogi, V.; Cheng, T.; Singh, A. Sustained Enzyme Activity of Organophosphorus Hydrolase in Polymer Encased Multilayer Assemblies. *Langmuir* **2003**, *19* (4), 1330–1336.

(22) Chen, B.; Lei, C.; Shin, Y.; Liu, J. Probing Mechanisms for Enzymatic Activity Enhancement of Organophosphorus Hydrolase in Functionalized Mesoporous Silica. *Biochem. Biophys. Res. Commun.* **2009**, *390* (4), 1177–1181.

(23) Lei, C.; Shin, Y.; Liu, J.; Ackerman, E. J. Entrapping Enzyme in a Functionalized Nanoporous Support. *J. Am. Chem. Soc.* **2002**, *124* (38), 11242–11243.

(24) LeJeune, K. E.; Russell, A. J. Biocatalytic Nerve Agent Detoxification in Fire Fighting Foams. *Biotechnol. Bioeng.* **1999**, *62* (6), 659–665.

(25) Pedrosa, V. A.; Paliwal, S.; Balasubramanian, S.; Nepal, D.; Davis, V.; Wild, J.; Ramanculov, E.; Simonian, A. Enhanced Stability of Enzyme Organophosphate Hydrolase Interfaced on the Carbon Nanotubes. *Colloids Surf., B* **2010**, *77* (1), 69–74.

(26) Mansee, A. H.; Chen, W.; Mulchandani, A. Detoxification of the Organophosphate Nerve Agent Coumaphos Using Organophosphorus Hydrolase Immobilized on Cellulose Materials. *J. Ind. Microbiol. Biotechnol.* **2005**, *32* (11–12), 554–560.

(27) Frančič, N.; Košak, A.; Lyagin, I.; Efrementko, E. N.; Lobnik, A. His6-OPH Enzyme-Based Bio-Hybrid Material for Organophosphate Detection. *Anal. Bioanal. Chem.* **2011**, *401* (8), 2631–2638.

(28) LeJeune, K. E.; Mesiano, A. J.; Bower, S. B.; Grimsley, J. K.; Wild, J. R.; Russell, A. J. Dramatically Stabilized Phosphotriesterase—Polymers for Nerve Agent Degradation. *Biotechnol. Bioeng.* **1997**, *54* (2), 105–114.

(29) Wei, W.; Du, J.; Li, J.; Yan, M.; Zhu, Q.; Jin, X.; Zhu, X.; Hu, Z.; Tang, Y.; Lu, Y. Construction of Robust Enzyme Nanocapsules for Effective Organophosphate Decontamination, Detoxification, and Protection. *Adv. Mater.* **2013**, *25* (15), 2212–2218.

(30) Novikov, B. N.; Grimsley, J. K.; Kern, R. J.; Wild, J. R.; Wales, M. E. Improved Pharmacokinetics and Immunogenicity Profile of Organophosphorus Hydrolase by Chemical Modification with Polyethylene Glycol. *J. Controlled Release* **2010**, *146* (3), 318–325.

(31) Sergeeva, V. S.; Efrementko, E. N.; Kazankov, G. M.; Gladilin, A. K.; Varfolomeev, S. D. Kinetic Behavior of Phosphotriesterase and Its Non-Covalent Complexes with Polyelectrolyte in Systems with Polar and Non-Polar Organic Solvents. *Biotechnol. Tech.* **1999**, *13* (7), 479–483.

(32) Mulchandani, P.; Chen, W.; Mulchandani, A. Microbial Biosensor for Direct Determination of Nitrophenyl-Substituted Organophosphate Nerve Agents Using Genetically Engineered *Moraxella* Sp. *Anal. Chim. Acta* **2006**, *568* (1–2), 217–221.

(33) Jha, R. K.; Kern, T. L.; Kim, Y.; Tesar, C.; Jedrzejczak, R.; Joachimiak, A.; Strauss, C. E. M. A Microbial Sensor for Organophosphate Hydrolysis Exploiting an Engineered Specificity Switch in a Transcription Factor. *Nucleic Acids Res.* **2016**, *44* (17), 8490–8500.

(34) Gilbert, E. S.; Walker, A. W.; Keasling, J. D. A Constructed Microbial Consortium for Biodegradation of the Organophosphorus Insecticide Parathion. *Appl. Microbiol. Biotechnol.* **2003**, *61* (1), 77–81.

(35) Jiang, J.; Zhang, R.; Li, R.; Gu, J.-D.; Li, S. Simultaneous Biodegradation of Methyl Parathion and Carbofuran by a Genetically Engineered Microorganism Constructed by Mini-Tn5 Transposon. *Biodegradation* **2007**, *18* (4), 403.

(36) Liu, Z.; Hong, Q.; Xu, J.-H.; Jun, W.; Li, S.-P. Construction of a Genetically Engineered Microorganism for Degrading Organophosphate and Carbamate Pesticides. *Int. Biodeterior. Biodegrad.* **2006**, *58* (2), 65–69.

(37) Hong, M. S.; Rainina, E.; Grimsley, J. K.; Dale, B. E.; Wild, J. R. Neurotoxic Organophosphate Degradation with Polyvinyl Alcohol Gel-Immobilized Microbial Cells. *Biorem. J.* **1998**, *2* (2), 145–157.

(38) Wang, A. A.; Mulchandani, A.; Chen, W. Specific Adhesion to Cellulose and Hydrolysis of Organophosphate Nerve Agents by a Genetically Engineered *Escherichia Coli* Strain with a Surface-Expressed Cellulose-Binding Domain and Organophosphorus Hydrolase. *Appl. Environ. Microbiol.* **2002**, *68* (4), 1684–1689.

(39) Shimazu, M.; Mulchandani, A.; Chen, W. Cell Surface Display of Organophosphorus Hydrolase Using Ice Nucleation Protein. *Biotechnol. Prog.* **2001**, *17* (1), 76–80.

(40) Mulchandani, A.; Rajesh. Microbial Biosensors for Organophosphate Pesticides. *Appl. Biochem. Biotechnol.* **2011**, *165* (2), 687–699.

(41) Jaffrezic-Renault, N. New Trends in Biosensors for Organophosphorus Pesticides. *Sensors* **2001**, *1*, 60.

(42) Saida, F.; Uzan, M.; Odaert, B.; Bontems, F. Expression of Highly Toxic Genes in *E. Coli*: Special Strategies and Genetic Tools. *Curr. Protein Pept. Sci.* **2006**, *7*, 47–56.

(43) Ras, M. R.; Borrull, F.; Marcé, R. M. Sampling and Preconcentration Techniques for Determination of Volatile Organic Compounds in Air Samples. *TrAC, Trends Anal. Chem.* **2009**, *28* (3), 347–361.

(44) Barker, Z.; Venkatchalam, V.; Martin, A. N.; Farquar, G. R.; Frank, M. Detecting Trace Pesticides in Real Time Using Single Particle Aerosol Mass Spectrometry. *Anal. Chim. Acta* **2010**, *661* (2), 188–194.

(45) Peng, Y.; Fu, S.; Liu, H.; Lucia, L. A. Accurately Determining Esterase Activity via the Isosbestic Point of P-Nitrophenol. *BioResources* **2016**, DOI: 10.15376/biores.11.4.10099-10111.

(46) Ngassa, G. B. P.; Tonlé, I. K.; Ngameni, E. Square Wave Voltammetric Detection by Direct Electroreduction of Paranitrophenol (PNP) Using an Organosmectite Film-Modified Glassy Carbon Electrode. *Talanta* **2016**, *147*, 547–555.

(47) Tapsoba, I.; Bourhis, S.; Feng, T.; Pontié, M. Sensitive and Selective Electrochemical Analysis of Methyl-Parathion (MPT) and 4-Nitrophenol (PNP) by a New Type p-NiTSPc/p-PPD Coated Carbon Fiber Microelectrode (CFME). *Electroanalysis* **2009**, *21* (10), 1167–1176.

(48) Liu, Y.; Cao, X.; Liu, Z.; Sun, L.; Fang, G.; Liu, J.; Wang, S. Electrochemical Detection of Organophosphorus Pesticides Based on Amino Acids-Conjugated P3TAA-Modified Electrodes. *Analyst* **2020**, *145* (24), 8068–8076.

(49) Qiu, L.; Lv, P.; Zhao, C.; Feng, X.; Fang, G.; Liu, J.; Wang, S. Electrochemical Detection of Organophosphorus Pesticides Based on Amino Acids Conjugated Nanoenzyme Modified Electrodes. *Sens. Actuators, B* **2019**, *286*, 386–393.

(50) Adkins, J. A.; Boehle, K.; Friend, C.; Chamberlain, B.; Bisha, B.; Henry, C. S. Colorimetric and Electrochemical Bacteria Detection

Using Printed Paper- and Transparency-Based Analytic Devices. *Anal. Chem.* **2017**, *89* (6), 3613–3621.

(51) Ru, S.-P.; Wu, J.; Ying, Y.-B.; Ji, F. Electrochemical Detection of Alkaline Phosphatase Using Ionic Liquid Modified Carbon Nanotubes Electrode. *Chin. J. Anal. Chem.* **2012**, *40* (6), 835–840.

(52) Kim, I.; Kim, G. H.; Kim, C. S.; Cha, H. J.; Lim, G. Optical Detection of Paraoxon Using Single-Walled Carbon Nanotube Films with Attached Organophosphorus Hydrolase-Expressed *Escherichia Coli*. *Sensors* **2015**, *15* (6), 12513–12525.

(53) Hayat, A.; Marty, J. L. Disposable Screen Printed Electrochemical Sensors: Tools for Environmental Monitoring. *Sensors* **2014**, *14* (6), 10432–10453.

(54) D'Souza, S. F. Microbial Biosensors. *Biosens. Bioelectron.* **2001**, *16* (6), 337–353.

(55) Belkin, S. Microbial Whole-Cell Sensing Systems of Environmental Pollutants. *Curr. Opin. Microbiol.* **2003**, *6* (3), 206–212.

(56) Joshi, N.; Wang, X.; Montgomery, L.; Elfick, A.; French, C. E. Novel Approaches to Biosensors for Detection of Arsenic in Drinking Water. *Desalination* **2009**, *248* (1), 517–523.

(57) Wang, B.; Barahona, M.; Buck, M. A Modular Cell-Based Biosensor Using Engineered Genetic Logic Circuits to Detect and Integrate Multiple Environmental Signals. *Biosens. Bioelectron.* **2013**, *40* (1), 368–376.

(58) Sagi, E.; Hever, N.; Rosen, R.; Bartolome, A. J.; Rajan Premkumar, J.; Ulber, R.; Lev, O.; Scheper, T.; Belkin, S. Fluorescence and Bioluminescence Reporter Functions in Genetically Modified Bacterial Sensor Strains. *Sens. Actuators, B* **2003**, *90* (1), 2–8.

(59) Ramanathan, S.; Shi, W.; Rosen, B. P.; Daunert, S. Sensing Antimonite and Arsenite at the Subattomole Level with Genetically Engineered Bioluminescent Bacteria. *Anal. Chem.* **1997**, *69* (16), 3380–3384.

(60) Breuer, M.; Rosso, K. M.; Blumberger, J.; Butt, J. N. Multi-Haem Cytochromes in *Shewanella Oneidensis* MR-1: Structures, Functions and Opportunities. *J. R. Soc., Interface* **2015**, *12* (102), 20141117.

(61) El-Naggar, M. Y.; Wanger, G.; Leung, K. M.; Yuzvinsky, T. D.; Southam, G.; Yang, J.; Lau, W. M.; Neilson, K. H.; Gorby, Y. A. Electrical Transport along Bacterial Nanowires from *Shewanella Oneidensis* MR-1. *Proc. Natl. Acad. Sci. U. S. A.* **2010**, *107* (42), 18127–18131.

(62) Von Canstein, H.; Ogawa, J.; Shimizu, S.; Lloyd, J. R. Secretion of Flavins by *Shewanella* Species and Their Role in Extracellular Electron Transfer. *Appl. Environ. Microbiol.* **2008**, *74* (3), 615–623.

(63) Marsili, E.; Baron, D. B.; Shikhare, I. D.; Coursolle, D.; Gralnick, J. A.; Bond, D. R. *Shewanella* Secretes Flavins That Mediate Extracellular Electron Transfer. *Proc. Natl. Acad. Sci. U. S. A.* **2008**, *105* (10), 3968–3973.

(64) Furst, A. L.; Hoepker, A. C.; Francis, M. B. Quantifying Hormone Disruptors with an Engineered Bacterial Biosensor. *ACS Cent. Sci.* **2017**, *3* (2), 110–116.

(65) Kaur, J.; Singh, P. K. Enzyme-Based Optical Biosensors for Organophosphate Class of Pesticide Detection. *Phys. Chem. Chem. Phys.* **2020**, *22* (27), 15105–15119.

(66) Dumas, D. P.; Caldwell, S. R.; Wild, J. R.; Raushel, F. M. Purification and Properties of the Phosphotriesterase from *Pseudomonas Diminuta*. *J. Biol. Chem.* **1989**, *264* (33), 19659–19665.

(67) Davis, R. J. Viability and Behavior of Lyophilized Cultures after Storage for Twenty-One Years. *J. Bacteriol.* **1963**, *85*, 486–487.

(68) Bowers, G. N. J.; McComb, R. B.; Christensen, R. G.; Schaffer, R. High-Purity 4-Nitrophenol: Purification, Characterization, and Specifications for Use as a Spectrophotometric Reference Material. *Clin. Chem.* **1980**, *26* (6), 724–729.

(69) Richins, R. D.; Mulchandani, A.; Chen, W. Enzymatic Characterization of Fusion Enzymes. *Biotechnol. Bioeng.* **2000**, *69*, 591.

(70) Efremenko, E. N.; Sergeeva, V. S. Organophosphate Hydrolase-An Enzyme Catalyzing Degradation of Phosphorus-Containing Toxins and Pesticides. *Russ. Chem. Bull.* **2001**, *50* (10), 1826–1832.

(71) Wise, A. A.; Kuske, C. R. Generation of Novel Bacterial Regulatory Proteins That Detect Priority Pollutant Phenols. *Appl. Environ. Microbiol.* **2000**, *66* (1), 163–169.

(72) Webster, D. P.; TerAvest, M. A.; Doud, D. F. R.; Chakravorty, A.; Holmes, E. C.; Radens, C. M.; Sureka, S.; Gralnick, J. A.; Angenent, L. T. An Arsenic-Specific Biosensor with Genetically Engineered *Shewanella Oneidensis* in a Bioelectrochemical System. *Biosens. Bioelectron.* **2014**, *62*, 320–324.

(73) Teravest, M. A.; Rosenbaum, M. A.; Kotloski, N. J.; Gralnick, J. A.; Angenent, L. T. Oxygen Allows *Shewanella Oneidensis* MR-1 to Overcome Mediator Washout in a Continuously Fed Bioelectrochemical System. *Biotechnol. Bioeng.* **2014**, *111* (4), 692–699.

(74) Kafi, A. K. M.; Chen, A. A Novel Amperometric Biosensor for the Detection of Nitrophenol. *Talanta* **2009**, *79* (1), 97–102.

(75) Santhiago, M.; Henry, C. S.; Kubota, L. T. Low Cost, Simple Three Dimensional Electrochemical Paper-Based Analytical Device for Determination of p-Nitrophenol. *Electrochim. Acta* **2014**, *130*, 771–777.

(76) Das, J.; Aziz, M. A.; Yang, H. A Nanocatalyst-Based Assay for Proteins: DNA-Free Ultrasensitive Electrochemical Detection Using Catalytic Reduction of p-Nitrophenol by Gold-Nanoparticle Labels. *J. Am. Chem. Soc.* **2006**, *128* (50), 16022–16023.

(77) Bretschger, O.; Obratsova, A.; Sturm, C. A.; In, S. C.; Gorby, Y. A.; Reed, S. B.; Culley, D. E.; Reardon, C. L.; Barua, S.; Romine, M. F.; et al. Current Production and Metal Oxide Reduction by *Shewanella Oneidensis* MR-1 Wild Type and Mutants. *Appl. Environ. Microbiol.* **2007**, *73* (21), 7003–7012.